SCIENTIFIC REPORTS

OPEN

Short term changes in the proteome of human cerebral organoids induced by 5-MeO-DMT

Received: 5 May 2017
Accepted: 14 September 2017
Published online: 09 October 2017

Vanja Dakic[1,2], Juliana Minardi Nascimento[1,3], Rafaela Costa Sartore[1,2], Renata de Moraes Maciel[1], Draulio B. de Araujo[4], Sidarta Ribeiro[4], Daniel Martins-de-Souza[3,5] & Stevens K. Rehen[1,2]

Dimethyltryptamines are entheogenic serotonin-like molecules present in traditional Amerindian medicine recently associated with cognitive gains, antidepressant effects, and changes in brain areas related to attention. Legal restrictions and the lack of adequate experimental models have limited the understanding of how such substances impact human brain metabolism. Here we used shotgun mass spectrometry to explore proteomic differences induced by 5-methoxy-N,N-dimethyltryptamine (5-MeO-DMT) on human cerebral organoids. Out of the 6,728 identified proteins, 934 were found differentially expressed in 5-MeO-DMT-treated cerebral organoids. *In silico* analysis reinforced previously reported anti-inflammatory actions of 5-MeO-DMT and revealed modulatory effects on proteins associated with long-term potentiation, the formation of dendritic spines, including those involved in cellular protrusion formation, microtubule dynamics, and cytoskeletal reorganization. Our data offer the first insight about molecular alterations caused by 5-MeO-DMT in human cerebral organoids.

Dimethyltryptamines are naturally-occurring molecules hypothesized to be involved in spontaneous altered states of consciousness such as dreams, free imagination, and insightful creativity[1,2]. N,N-dimethyltryptamine (N,N-DMT) and bufotenine (5-HO-DMT) have been traditionally used as entheogens by Amerindians[3,4] as major active ingredients of *Virola* snuff and a brew called *Ayahuasca*[5]. The popularity of *Ayahuasca* as part of religious ceremonies continues to spread in South America and other countries[6], possibly motivated by its strong antidepressant effects[7,8]. Chronic *Ayahuasca* ingestion has been associated with cognitive gains and structural brain changes in areas related to attention, self-referential thought, and internal mentation[9,10]. Another member of this group of molecules is 5-methoxy-N,N-dimethyltryptamine (5-MeO-DMT), secreted in large amounts by *Incilius alvarius*[11,12]. 5-MeO-DMT has been used more recently by the Seris, an indigenous group from the state of Sonora, in Mexico.

The search for the molecular mechanisms underlying the effects of dimethyltryptamines showed that N,N-DMT and 5-MeO-DMT, two closely related metabolic products, can act as systemic endogenous regulators of inflammation and immune homeostasis through both 5-hydroxytryptamine receptors (5-HTRs) and sigma-1 receptors (σ-1Rs)[13,14]. Under severe hypoxia, N,N-DMT robustly increased the survival of *in vitro* cultured human cortical neurons, monocyte-derived macrophages, and dendritic cells acting through σ-1Rs[15]. The direct evidence of neuroimmune communication and neuroregenerative effects of N,N-DMT and 5-MeO-DMT greatly enhanced expectations for psychedelic research.

Our limited understanding of the physiological activity of dimethyltryptamines and other classic psychedelic substances is caused not only by legal restrictions on such research[16,17] but also by the lack of adequate experimental models[18–20]. In the past few years, considerable progress has been made regarding the neural differentiation of human pluripotent stem cells into mature neurons and cerebral organoids[21]. Human neural

[1]D'Or Institute for Research and Education (IDOR), Rio de Janeiro, Brazil. [2]Institute of Biomedical Sciences, Federal University of Rio de Janeiro, Rio de Janeiro, Brazil. [3]Laboratory of Neuroproteomics, Institute of Biology, Department of Biochemistry and Tissue Biology, University of Campinas (UNICAMP), Campinas, Brazil. [4]Brain Institute, Federal University of Rio Grande do Norte, Natal, Brazil. [5]Instituto Nacional de Biomarcadores em Neuropsiquiatria (INBION), Conselho Nacional de Desenvolvimento Cientifico e Tecnologico, Sao Paulo, Brazil. Vanja Dakic and Juliana Minardi Nascimento contributed equally to this work. Correspondence and requests for materials should be addressed to S.K.R. (email: srehen@lance-ufrj.org)

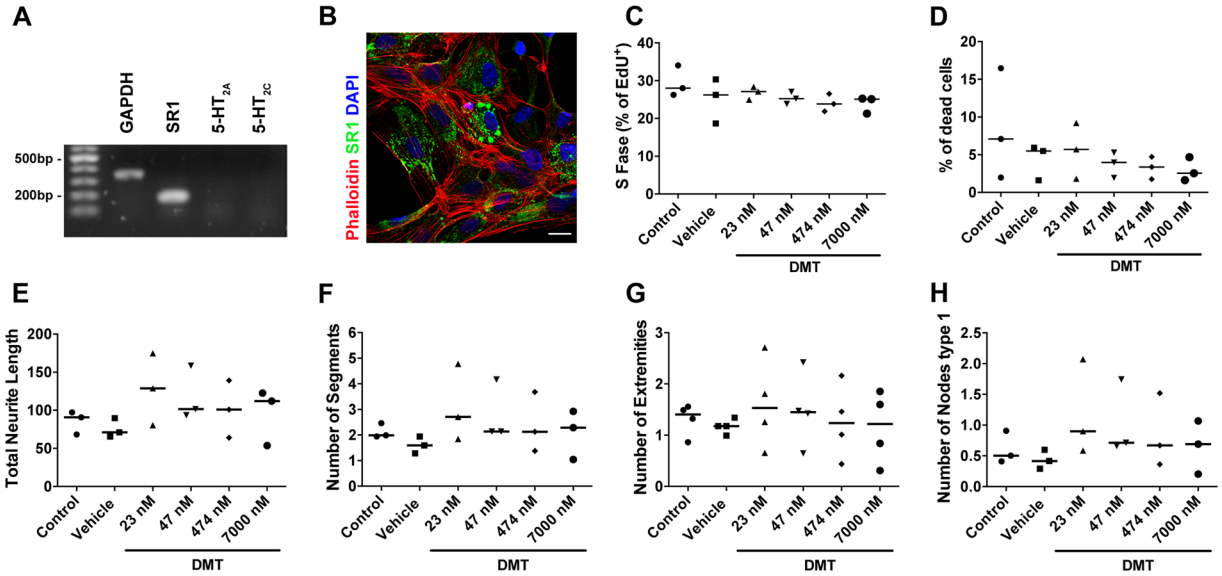

Figure 1. Effects of 5-MeO-DMT on hNPCs. **(A)** Expression of mRNA for internal control (GAPDH), SR1, 5-HT_{2A}, and 5-HT_{2C} in hNPCs. **(B)** Confirmation of σ-1R protein (green) expression by immunocytochemistry, phalloidin showing the cytoskeleton (red) and DAPI staining nuclei (blue), scale bar 20 μm. **(C)** Quantification of cell proliferation based on EdU staining after treatment with 5-MeO-DMT. **(D)** Percentage of dead cells in hNPCs treated with 5-MeO-DMT. **(E–H)** Effects of 5-MeO-DMT on neuronal arborization by quantification of **(E)** total neurite length (sum of the length of all neurites attached to the cell), **(F)** number of segments, **(G)** number of extremities, and **(H)** number of nodes type 1. Bar represents median. Data were analyzed by one-way ANOVA with Tukey's multiple comparison test, and only p-values < 0.05 were considered significant. Here, all comparisons showed p-values > 0.05.

progenitor cells (hNPC) are useful cell systems for high-throughput screening due to their homogeneity, along with little complexity and limited differentiation potential. On the other hand, cerebral organoids are complex, three-dimensional (3D) culture systems composed of multiple cell types that self-organize into various brain regions similarly to those *in vivo*, including the cerebral cortex, ventral forebrain, midbrain–hindbrain boundary, and hippocampus[22,23]. Combining different cell types in a complex 3D configuration can better simulate brain biology and function. As such, cerebral organoids can reproduce the function and architecture of the brain, especially regarding development and neuronal plasticity. A comparison of gene expression programs of human fetal neocortex and *in vitro* cortical development by single-cell RNA sequencing found remarkable similarities[24]. Cerebral organoids may well recapitulate environmental effects on human nervous system, particularly related to plasticity and growth[24–26], and circumvent problems of discrepancies in metabolic pathways occurring in translational studies involving animal models. The development of such a model offers an exciting new range of opportunities to investigate the molecular responses of human neural tissue to psychoactive substances.

Here we analyzed the effect of 5-MeO-DMT on human neural cells and cerebral organoids. By employing mass spectrometry-based proteomics to analyze cerebral organoids, we managed to investigate effects on a large scale and in an unbiased manner, and also gained insight into its molecular mechanisms and biochemical pathways[27]. To the best of our knowledge, our results are the first to show that 5-MeO-DMT modulates proteins involved in long-term potentiation (LTP), in addition to morphogenesis and maturation of dendritic spines, while inhibiting neurodegeneration and cell death.

Results

Human neural progenitor cells are unaffected by 5-MeO-DMT. First, we examined the effects of 5-MeO-DMT on hNPCs (detailed characterization in[28]). hNPCs showed basal expression of σ-1Rs but not 5-HT_{2A} or 5-HT_{2C} receptors (Fig. 1A,B). Using a high-content screening analysis, we tested the effects of 5-MeO-DMT (23 nM to 7.11 μM) on hNPC death, proliferation, and differentiation. There was no evidence of change in cell death or proliferation in response to 5-MeO-DMT (Fig. 1C,D). In addition, by quantifying some aspects of dendritic branch complexity, we measured neural arborization based on MAP2 staining of young neurons exposed to 5-MeO-DMT compared to an unexposed control. Despite a slight trend, there were no statistically significant differences in the measured parameters (Fig. 1E–H, all $p > 0.05$).

Human cerebral organoids express 5-MeO-DMT receptors. The lack of alterations in cell death, proliferation, and differentiation/arborization in hNPCs exposed to 5-MeO-DMT could be due to the low cellular diversity and lack of complex interactions between different cell types. Thusly, we tested human cerebral organoids, which better replicate the complexity and function of *in vivo* neural circuitry. In 45 day-old cerebral organoids, basal immunostaining was observed in AMPA (selective glutamate receptor 2) and NMDA (ionotropic glutamate receptor) – both characteristic of glutamatergic synapses – along with the neuronal marker MAP2

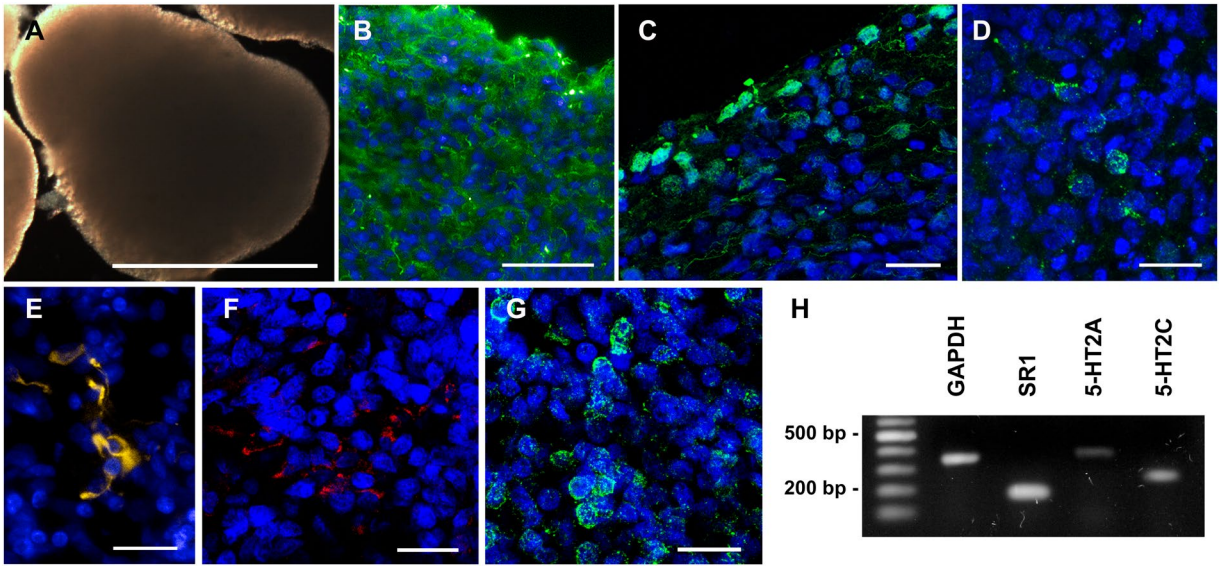

Figure 2. Cerebral organoids express 5-MeO-DMT receptors and different cell type markers. **(A)** Cerebral organoids presenting smooth texture and homogeneous coloring at 45 days of differentiation (scale bar 1000 μm). **(B)** Cerebral organoids are composed of several cell types, including mature neurons, as shown by MAP2 staining. **(C)** Cells expressing AMPAR1 are found at the organoid edge, while **(D)** cells expressing NMDAR1 and **(E)** GFAP are detected within the organoid. **(F)** Cells positive for 5-HT_{2A} receptor, and **(G)** σ-1R, the primary molecular targets for 5-MeO-DMT, are also found in the organoid. Scale bars: A = 1000 μm; B = 50 μm; C, D, E, F, and G = 20 μm. **(H)** The expression of molecular targets for 5-MeO-DMT was also confirmed by RT-PCR.

(Fig. 2A–D), as previously described[29]. Glial cells (GFAP+) are also present in organoids, as shown in Fig. 2E. Interestingly, in contrast with hNPCs, we were able to detect the expression of the 5-HT_{2A} receptor via PCR and/or immunostaining, as well as of σ-1Rs, the primary pharmacological molecular targets for 5-MeO-DMT. As shown in Fig. 2F,G, cells expressing the 5-HT_{2A} receptor are present within the cerebral organoid, and the sigma-1 receptor was detected as well. RT-PCR confirmed the expression of 5-HT_{2A} and σ-1 receptors, and allowed the detection of serotonin 5-HT_{2C} receptors as well (Fig. 2H). Taken together, these data validate cerebral organoids as an appropriate platform to seek for the effects of 5-MeO-DMT in an amenable and realistic human neuronal network.

5-MeO-DMT alters the proteome of human cerebral organoids. Due to the complexity of the organoid system, we decided to cast a much wider net to detect potentially important 5-MeO-DMT effects. By analyzing the proteome of organoids with and without treatment, we were able to look for changes in the expression of a considerable number of proteins, in an unbiased approach. Thus, to resolve the proteome of human neural tissue under the effect of 5-MeO-DMT, we analyzed 45-day-old cerebral organoids after 24-hour treatment (Fig. 3A). A total of 144,700 peptides were identified at a false discovery rate (FDR) below 1%. These led to the identification of 6,728 unique proteins by, at least, two unique peptides present in no less than two out of three biological replicates analyzed. Notably, there was an overlap of 99% of identified proteins among all treatment groups (Fig. 3B), demonstrating the robustness of the method. From these commonly identified proteins, we found 934 differentially expressed (using a $-2 < \mathrm{Log}_2$ ratio > 2 cut-off), comprising 360 downregulated and 574 upregulated proteins when comparing 5-MeO-DMT and vehicle groups (an overview of the proteomics results is presented in Supplementary Table 1). Functional enrichment for combined up- and downregulated proteins predicted the biological functions of those changes. Regarding diseases or functions, using prediction effect analysis ($-2 <$ z-score > 2.0 is significant for inhibition/activation) (Fig. 3C), we observed a significant activation score for dendritic spine and cellular protrusion formation, microtubule and cytoskeletal organization, and also mild activation of T lymphocyte differentiation. On the other hand, biological functions such as neurodegeneration, cell death, and brain lesion were predicted to be inhibited.

5-MeO-DMT leads to inhibition of NF-κB signaling pathway. Among the canonical pathways identified are nuclear factor of activated T-cells (NFAT) and nuclear factor kappa B (NF-κB) signaling via toll-like receptor (TLR) and Gq-coupled receptors, which are all inhibited by 5-MeO-DMT treatment (Fig. 4). Interestingly, the direct targets of 5-MeO-DMT, receptors 5-HT_{2A} and 5-HT_{2C}, are Gq-coupled. Furthermore, NF-κB is very well known to be the main transcriptional regulator of inflammatory, pro-inflammatory and anti-inflammatory cytokines and chemokines[14].

Proteins associated with long-term potentiation are modulated by 5-MeO-DMT. We have also identified regulation of specific proteins that participate in LTP, one of the main properties of most excitatory synapses throughout the CNS[30]. Proteins found upregulated are NMDAR, CaMK2 (Ca^{2+}/calmodulin-dependent

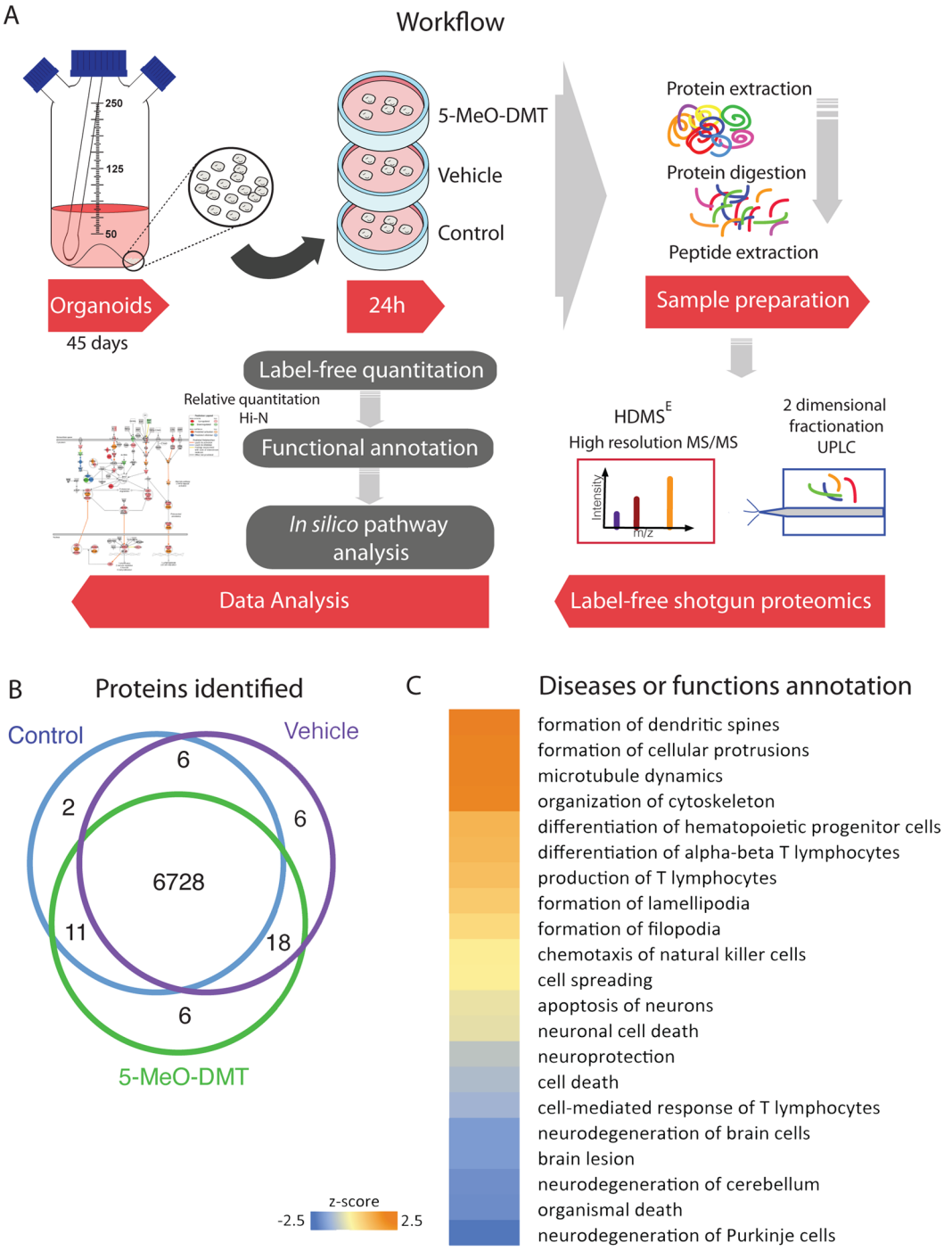

Figure 3. 5-MeO-DMT treatment effects on human cerebral organoid proteomics. **(A)** Experimental design workflow. 45-day-old cerebral organoids were treated with either 5-MeO-DMT, vehicle, or left untreated for 24 h. Samples were analyzed using label-free state-of-the-art quantitative proteomics, using two-dimensional fractionation and high-resolution mass spectrometry. Workflow art was modified from[29]. **(B)** Venn diagram comparing the number of proteins identified by shotgun mass spectrometry in control human cerebral organoids, those treated with vehicle (EtOH), and 5-MeO-DMT. **(C)** Heat map showing significant functional enrichment between 5-MeO-DMT versus vehicle human cerebral organoids.

protein kinase), and CREB (cyclic AMP-responsive element-binding protein). The group of downregulated proteins included mGluR5 (metabotropic glutamate receptor 5), $G_{\alpha q}$ protein, protein kinase C (PKC), phospholipase c (PLC), calmodulin (CaM), AC1/8, inositol 1,4,5-trisphosphate receptor (IP3R), exchange factor directly activated by cAMP 1 (EPAC1) and PKA (protein kinase A). These changes in key components, and further regulation of several other proteins and secondary messengers suggest a complex regulation of this pathway. AMPAR, and the signaling cascade leading to c-Raf, mitogen-activated protein kinase kinase 1/2 (MEK1/2), and extracellular regulated kinase

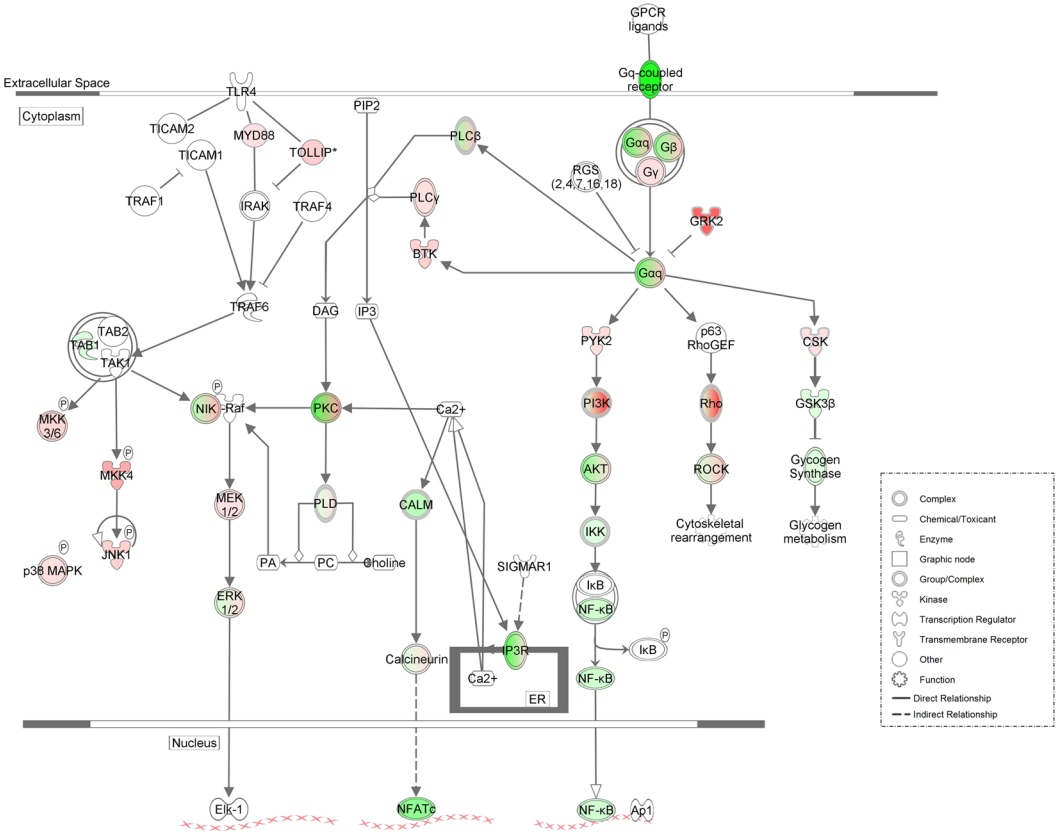

Figure 4. Schematic representation of the changes in protein expression of NFAT and NF-κB pathways by 5-MeO-DMT. Canonical pathways showing upregulated (red) and downregulated proteins (green) after 5-MeO-DMT treatment.

1/2 (ERK1/2) are upregulated, suggesting pathway activation (Fig. 5). Based on the literature, activated ERK1/2 is transported to the nucleus and activates CREB, resulting in the expression of a large number of downstream genes[31].

Cytoskeletal reorganization and dendritic spine morphogenesis proteins altered by 5-MeO-DMT. Ephrin B was another canonical pathway upregulated, including both forward and reverse signaling, as shown by the analysis of differentially expressed proteins (see Fig. 6). Upregulation of ephrin-B2 causes activation of ephrin type-B receptor (EPHB) and, through intersectin, activates a cascade including CDC42 (cell division control protein 42 homolog), N-WASP (neural Wiskott-Aldrich syndrome protein), and ARP2/3 (actin-related protein 2/3). This upregulation additionally activates RAC1 (Ras-related C3 botulinum toxin substrate 1) through ELMO1. Together, these activated pathways trigger dynamic reorganization of the actin cytoskeleton and dendritic spine morphogenesis in forward signaling[32]. Meanwhile reverse signaling activates plexin, a protein that acts as a receptor for semaphorin through NCK adaptor protein 2 (GRB4) and focal adhesion kinase (FAK), causing axonal repulsion through paxillin (PXN).

Additionally, we found significant regulation of plexins, integrins, SLIT-ROBO Rho GTPase-activating protein (srGAP), Netrin receptor DCC, and metalloproteinase (Table 1) in 5-MeO-DMT-treated cerebral organoids, which corroborates actin regulation and orchestrates cytoskeletal reorganization.

Discussion

5-MeO-DMT is a structural analog of serotonin and melatonin and a functional analog of other psychedelic tryptamines such as N,N-DMT and 5-HO-DMT, a group of molecules about which little is known. The present results suggest that 5-MeO-DMT modulates the anti-inflammatory response, as well as the formation and maturation of new dendritic spines, via proteins implicated with cellular protrusion formation, microtubule dynamics, cytoskeletal reorganization, and LTP. These changes were observed in the organoids but not in monolayer cultures of neuronal cells, which suggests a more mature and complex 3D circuitry is necessary for the actions of 5-MeO-DMT.

Here we demonstrate anti-inflammatory effects of 5-MeO-DMT using human cerebral organoids. NFAT and NF-κB signaling pathways were shown to be downregulated via Toll-like receptors (TLR) and Gq-coupled protein receptors, most probably 5-HT_{2A} and 5-HT_{2C}. Anti-inflammatory effects of 5-MeO-DMT were previously reported on human monocyte-derived dendritic cells, where inflammatory cytokine and chemokine release was shown to be blocked[14]. The immunomodulatory potential of other serotonergic psychedelics like lysergic acid diethylamide (LSD)[33,34], 3,4-methylenedioxy-methamphetamine (MDMA)[35,36], and

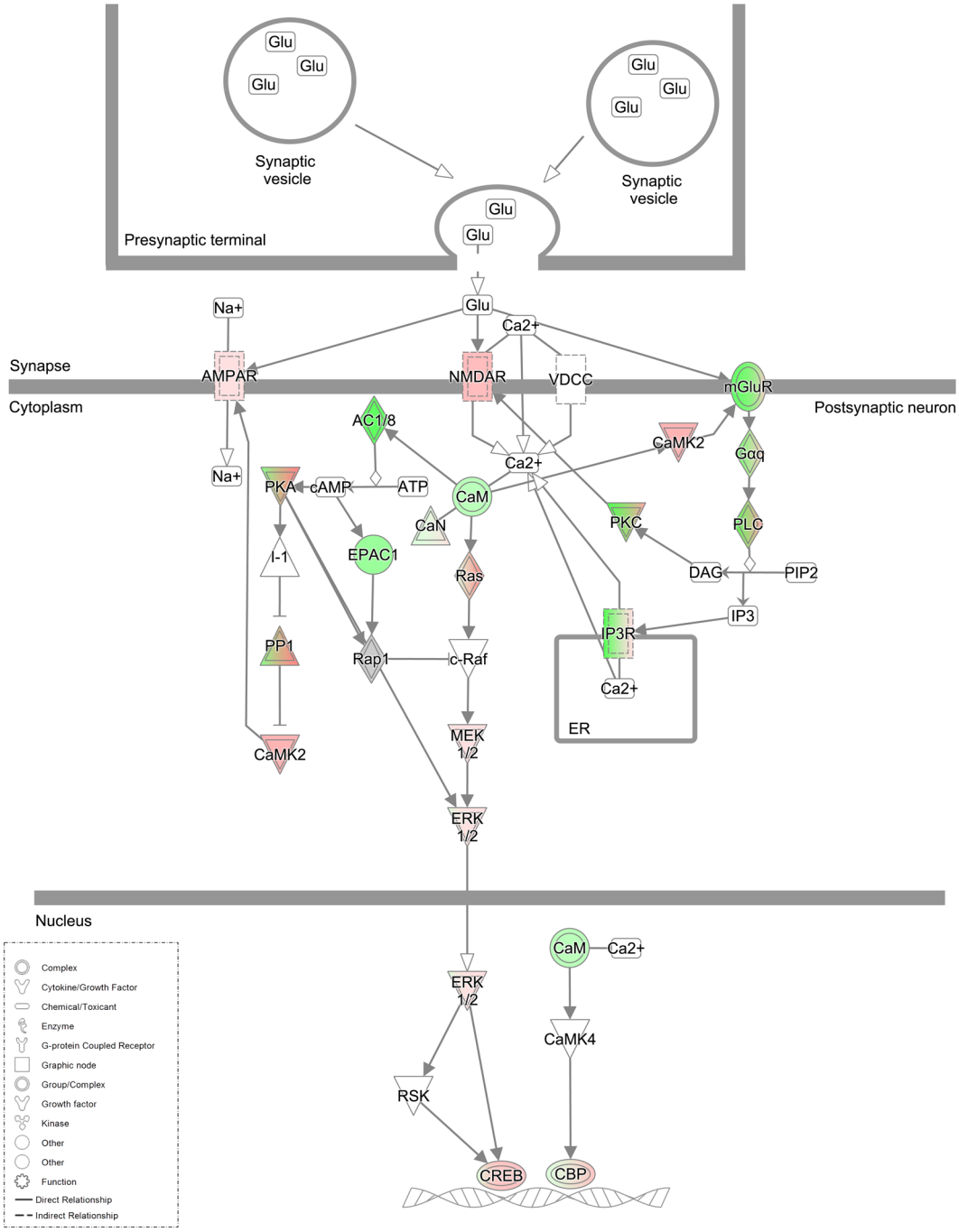

Figure 5. Schematic representation of long term potentiation modulation by 5-MeO-DMT treatment. Z-scores were calculated from an upstream shortest-path analysis and gave the probability that the interaction between the proteins and the common regulator is not occurring by chance. In red, upregulated proteins; in green, downregulated proteins after 5-MeO-DMT treatment. Glu, glutamate.

2,5-dimethoxy-4-iodoamphetamine (DOI)[37,38] were also previously reported. It is hypothesized that there is cross-talk between TLR, serotonin receptors, and σ-1Rs[39].

Our work also suggests that a single, 24-hour-treatment with 5-MeO-DMT, i.e., a single dose, modulates specific signaling molecules identified as key players in LTP, a classic mechanism of learning and memory[30]. Based on *in silico* predictions using proteomic data, modulation of these signaling molecules by 5-MeO-DMT would produce a complex regulation of LTP. One possibility is that LTP may be augmented in some cell types and inhibited in others, leading to a mixed profile, however; functional studies such as electrophysiology were not performed.

Additionally, we observed major downregulation of mGluR5 after treatment with 5-MeO-DMT. mGluR5 has a role in the rewarding effects for several drugs of abuse. It was shown that mice lacking the mGluR5 gene do not self-administer cocaine and show no cocaine-induced hyperactivity[40]. They also have attenuated somatic signs

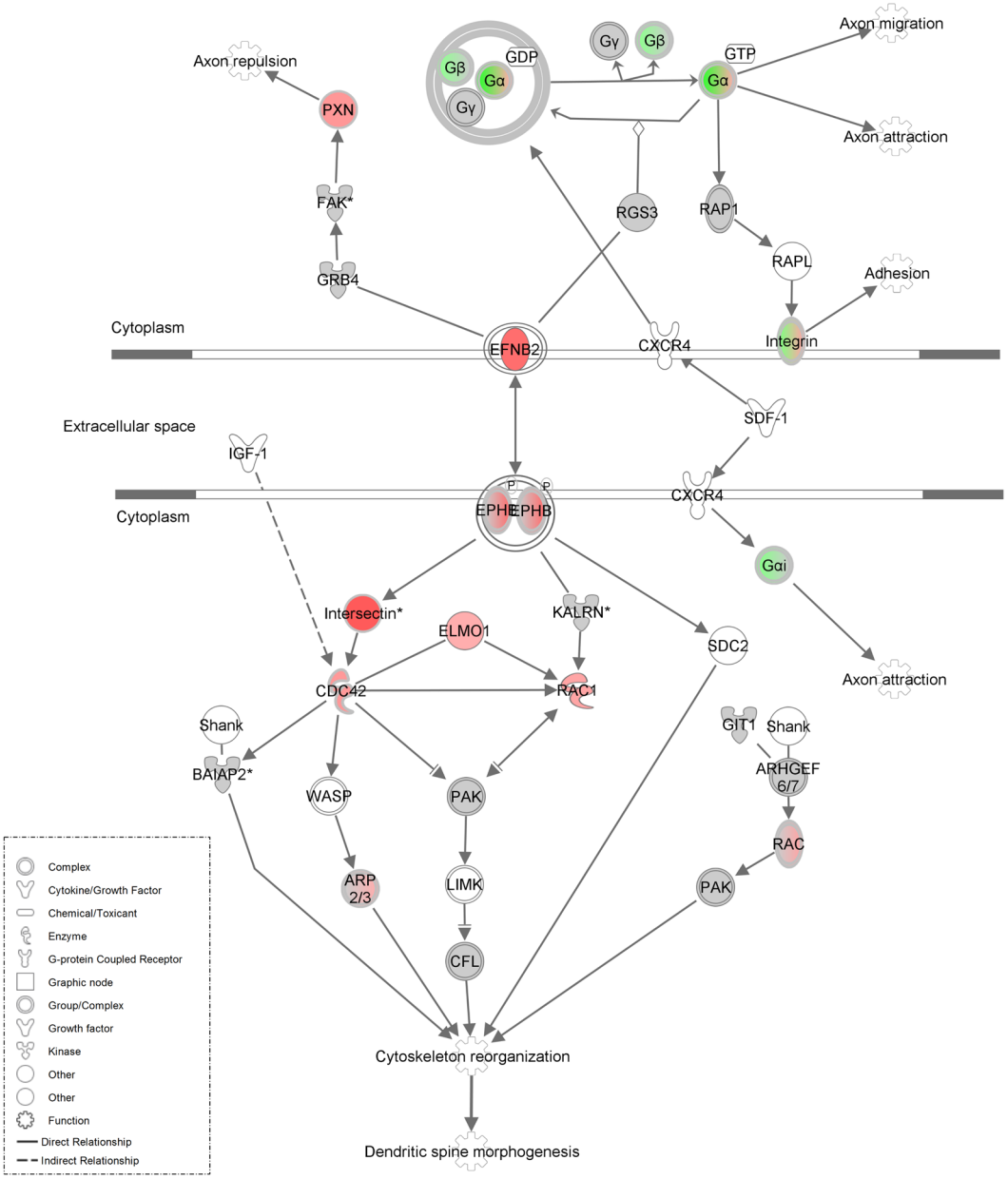

Figure 6. Pathway showing influence of 5-MeO-DMT on cytoskeletal reorganization and dendritic spine morphogenesis. Canonical pathway showing upregulated (red) and downregulated (green) proteins.

of nicotine withdrawal[41], and reduced ethanol consumption behavior[42], suggesting mGluR5 may be involved in addiction. The same effect for cocaine, nicotine, and ethanol in rats has been demonstrated with the use of mGlu5 receptor antagonists[41]. These effects of 5-MeO-DMT can possibly explain the therapeutic effect of dimethyltryptamines *from Ayahuasca* on substance dependence[3,43–47]. Moreover, *Ayahuasca* seems to inhibit addictive behaviors in an animal model of alcohol dependence[16]. In humans, Ayahuasca administration to healthy subjects reduces rapid-eye-movement sleep (REM) and increases slow-wave sleep (SWS)[48], two major sleep stages respectively associated with increased and decreased LTP[49–52], while producing dream-like effects. Thus, the complex regulation of LTP detected here may also indicate that 5-MeO-DMT produces a mix of SWS and REM-like effects.

Changes in LTP are directly associated with increase in dendritic spine number and size; and conversely, changes in LTD are associated with a decrease in number and size[53]. Spine morphogenesis relies on alterations of the actin cytoskeleton, but the molecular mechanisms that regulate this process are still not clear. 5-MeO-DMT caused significant upregulation of EFNB2, EPHB, and various secondary messengers involved in dendritic spine formation. Dendritic spine formation can be induced by direct stimulation of serotonergic receptors. Indeed the selective 5-HT_{2A} receptor agonist, DOI, has been shown to modulate spine morphology of mature cortical pyramidal neurons[54]. In this study, a transient increase in spine size induced by DOI was kalirin-dependent, and it enhanced phosphorylation of PAK; whereas here we show upregulation of EFNB2, EPHB, intersectin, ELMO1, CDC42, and RAC1. Binding of ephrin-B to EphB receptors initiates bidirectional signaling, which by altering the

Accession Integrins	Gene Name	Peptide count	Description	Log_2 Ratio
O95965	ITGBL1	4 (2)	Integrin beta-like protein 1	3.69
P23229	ITGA6	21 (3)	Integrin alpha-6	3.18
P13612	ITGA4	10 (5)	Integrin alpha-4	2.57
P16144	ITGB4	42 (12)	Integrin beta-4	1.66
P11215	ITGAM	8 (3)	Integrin alpha-M	1.65
P20701	ITGAL	8 (3)	Integrin alpha-L	1.36
P05556	ITGB1	34 (15)	Integrin beta-1	1.26
P38570	ITGAE	16 (3)	Integrin alpha-E	1.10
P26006	ITGA3	22 (4)	Integrin alpha-3	0.69
Q9H0C8	ILKAP	13 (6)	Integrin-linked kinase-associated serine/threonine phosphatase 2 C	0.26
Q969R8	ITFG2	3 (2)	Integrin-alpha FG-GAP repeat-containing protein 2	−0.99
P20702	ITGAX	5 (1)	Integrin alpha-X	−1.53
P06756	ITGAV	16 (7)	Integrin alpha-V	−2.08
Q13683	ITGA7	10 (3)	Integrin alpha-7	−2.32
P17301	ITGA2	19 (2)	Integrin alpha-2	−2.64
Netrins and Plexins				
Q9ULL4	PLXNB3	19 (5)	Plexin-B3	0.71
O43157	PLXNB1	10 (2)	Plexin-B1	0.33
Q8NEU8	APPL2	37 (11)	DCC-interacting protein 13-beta	−0.30
Q9UKG1	APPL1	43 (21)	DCC-interacting protein 13-alpha	−0.41
O15031	PLXNB2	156 (45)	Plexin-B2	−2.14
P43146	DCC	50 (8)	Netrin receptor DCC	−4.51
Semaphorins				
Q13214	SEMA3B	14 (4)	Semaphorin-3B	2.11
Q13591	SEMA5A	16 (4)	Semaphorin-5A	−1.66
Q8NFY4	SEMA6D	8 (2)	Semaphorin-6D	−1.69
Q9NPR2	SEMA4B	15 (3)	Semaphorin-4B	−1.82

Table 1. Table of proteins showing regulation of integrins, netrins, plexins, and semaphorins by 5-MeO-DMT.

actin cytoskeleton, leads to changes in dendritic spine shape, size, and number[55]. It was shown that EPHB2 interacts with intersectin and activates its GEF activity in cooperation with N-WASP, which in succession activates the Rho-family GTPase Cdc42 and spine morphogenesis[56]. N-WASP is a critical regulator of Arp2/3-mediated actin polymerization[57]. Henkemeyer and colleagues[58] demonstrated that triple EphB1,2,3-deficient hippocampal neurons have abnormal formation of actin clusters along dendrites, impairing normal dendritic spine formation *in vivo*. Meanwhile, *in vitro*, knockdown of EphB2 alone is sufficient to reduce synapse density[59]. Postnatal re-expression of EphB2 in slice cultures from animals lacking EphB1–3 is sufficient to rescue dendritic spine defects[59]. Although EphB signaling has a clear role in dendritic spine morphogenesis through kinase domain activity, it can also regulate activity-dependent synaptic plasticity interacting with both NMDA[60] and AMPA receptors[59]. Literature shows that σ-1R also could contribute to the brain plasticity effects of 5-MeO-DMT. σ-1R is an endogenous regulator of dendritic spine morphology[61,62] and neurite outgrowth[61].

Typical psychological effects of psychedelics such as changes in perception and thought, renewed sensation of novelty, ineffability, and awe[63] may derive directly from the strong modulation of synaptic and cellular plasticity promoted by 5-MeO-DMT, and putatively compounds of other classical psychedelics. Given the pathways activated, the psychological effects of 5-MeO-DMT must also be tightly linked to the millisecond changes in sub-membrane calcium metabolism. To test these hypotheses, however, it would be necessary to go beyond *in vitro* studies to investigate in detail the links between the acute and chronic effects of 5-MeO-DMT.

Recently, organoid models have been used to study neural progenitor dysfunction and progenitor abnormalities resulting, for example, from Zika virus infections[23,25]. The scientific community is still exploring the broader application of brain organoids. Beyond modeling early events of progenitor biology, brain organoids have the potential to model higher-order functions of the human brain, such as cellular interactions and neural circuit dysfunctions[23,64].

Apart from acting as a direct molecular mediator of plasticity, 5-MeO-DMT had effects on cell surface and extracellular proteins involved in regulating synaptic architecture, like plexins[65], DCC[66], metalloproteinase[67], and integrins[68,69]. An upregulation of integrins, as we observed here in 5-MeO-DMT-treated organoids, was also found in major depressive disorder patients who responded well to antidepressants, suggesting the importance of this class of proteins in brain plasticity[70]. One more protein significantly downregulated is srGAP, an intracellular

signaling molecule with a role in processes underlying synaptic plasticity, higher cognitive function, learning, and memory[71].

Finally, we also found that pathways, associated with cell death, in brain organoids were inhibited by 5-MeO-DMT. These neurorestorative and cellular protective effects are expected upon activation of σ1R[15,72]. σ1R agonists exert neuroprotective effects by regulating intracellular calcium levels[73], preventing expression of pro-apoptotic genes[74], and protecting mRNA against anti-apoptotic genes such as Bcl-2.

Fast antidepressants also have strong effect on synaptic plasticity, reversing functional and structural synaptic deficits caused by stress. A typical example of this group is ketamine, a hallucinogenic, non-competitive NMDA glutamate receptor channel antagonist, which causes an improvement in mood ratings within hours, as opposed to weeks as seen in typical antidepressants[75]. Ketamine increases mammalian target of rapamycin complex 1 (mTORC1) signaling, via activation of protein kinase B (PKB or Akt) and ERK. mTOR signaling then boosts synaptic protein synthesis and spine stability and function in the prefrontal cortex[75–77].

Whereas other dimethyltryptamines could have similar effects, our results do not support that this is common to actions of other dimethyltryptamines or non-psychoactive tryptamines, which should be examined independently. Taken together, our data offer insight about molecular changes induced by 5-MeO-DMT in human cerebral organoids. The proteomic profile, observed after exposure to 5-MeO-DMT, points to actions on synaptic plasticity and cell survival in human brain organoids.

Materials and Methods

Human embryonic stem cells. BR1 lineage of human embryonic stem cells (hESCs)[78] was cultured in mTeSR1 media (Stemcell Technologies) on Matrigel (BD Biosciences) - coated surface. The colonies were manually passaged every seven days and maintained at 37 °C in humidified air with 5% CO_2.

Human neural progenitor cells. To induce hESCs towards neural differentiation, we adapted Baharvand and coworkers' protocol[28,79]. Briefly, 70% confluent human embryonic stem cells were differentiated to the neural lineage in defined adherent culture by retinoic acid and basic fibroblast growth factor (bFGF) within 18 days of culture. On the 18th day, neural tube-like structures were collected and plated on dishes coated with 10 μg/mL of poly-L-ornithine and 2.5 μg/mL of laminin (Thermo Fisher Scientific). The population of human neural progenitor cells (hNPCs) that migrated from neural tube-like structures was tested for the expression of neuronal markers and expanded. Expansion was done in N2B27 medium supplemented with 25 ng/mL bFGF and 20 ng/mL EGF (Thermo Fisher Scientific). N2B27 medium consisted of DMEM/F-12 supplemented with 1X N2, 1X B27, 1% penicillin/streptomycin (Thermo Fisher Scientific). Cells were incubated at 37 °C and 5% CO_2. Medium was replaced every other day. hNPCs were expanded for no more than 5 passages. Basic characterization of this culture was published in[28].

High Content Screening. Cell proliferation, cell death and arborization experiments were performed in a High Content Screening (HCS) format. hNPCs (1,500 cells per well) were plated on a 384-multiwell μClear plate (Greiner Bio-One, Kremsmünster, Austria) coated with 100 μg/mL poly-L-ornithine and 10 μg/mL laminin (Thermo Fisher Scientific). After 24h, cells were treated for 4 days in quintuplicate (five wells per condition) with 5-MeO-DMT (Sigma-Aldrich) in N2B27 medium supplemented with bFGF and EGF. Cells were labeled with 10 μM EdU for 2h min prior to fixation and image acquisition. For the cell death assessment, cells were labeled with LIVE/DEAD® viability/cytotoxicity kit (Thermo Fisher Scientific). This kit contains two probes: calcein AM and ethidium homodimer (EthD-1). The former allows measuring of intracellular esterase activity and the latter, plasma membrane integrity. Mixing of probes was done in DMEM/F-12 (without phenol red, Life Technologies), together with the cell-permeant nuclear dye Hoechst. After incubation for 30 min at 37 °C and 5% CO_2, the dye cocktail was replaced by new medium and images were acquired. For arborization experiments, neural differentiation was induced 24h after plating by removal of bFGF and EGF from N2B27 medium. Treatment with 5-MeO-DMT was done concomitantly with neural differentiation. Medium was changed after 4 days of treatment and cells were allowed to differentiate for 3 more days. On day 7 cells were fixed for immunocytochemistry.

High Content Analysis. All images were acquired on Operetta high-content imaging system (Perkin Elmer, USA). For proliferation, incorporated EdU was detected with Alexa Fluor 488 using Click-iT EdU kit (C10351, Invitrogen, Carlsbad, USA) following the manufacturer's instructions. Total number of cells was calculated by nuclei stained with 1 mg/mL of DAPI (4',6-diamidino-2-phenylindole). S phase was determined by percentage of total cells labeled with EdU. Images were acquired with a 10x objective with high numerical aperture (NA).

Live cell imaging was performed with LIVE/DEAD® viability/cytotoxicity kit, using temperature and CO_2 control option (TCO) of Operetta, set to 37 °C and 5% CO_2 at 10x magnification. Quantification analyses were normalized to the number of cells in the well segmented by nucleus dyes.

Neuronal arborization was evaluated of fixed cells stained for MAP2 after 7 days of differentiation. The images were analyzed using the Neurite Outgrowth script of the Harmony software. Briefly, neurites were detected on MAP2 positive cells using the Find Neurite building block, which provides a dedicated algorithm for segmenting neurites. Morphological characteristics of neuronal arborization, such as total neurite length (sum of the length of all neurites attached to the cell), number of extremities, number of segments, and number of nodes (type I) were defined based on selected threshold parameters of the Find Neurite building block.

All analysis sequences were designated by combining segmentation steps with morphological- and fluorescence-based object characterizations using the image analysis software Harmony 3.5.1 (Perkin Elmer, Waltham, MA, USA).

Differentiation into cerebral organoids. Differentiation of hESCs into cerebral organoids was based on a previously described protocol[26,29]. Briefly, hESC cells were inoculated into a spinner flask, and to enable embryoid body formation, after six days the medium was changed to neural induction media (DMEM/F12, 1X N2 supplement (Gibco), 2 mM Glutamax (Invitrogen), 1% MEM-NEAA, and 1 μg/mL heparin (Sigma)) and the aggregates were cultured for five more days. After being embedded in matrigel, differentiation media composed of 1:1 DMEM/F12:Neurobasal (Gibco), 0.5X N2, 1X B27 minus vitamin A (Gibco), 2 mM Glutamax, 0.5% MEM-NEAA, 0.2 μM 2-mercaptoethanol and 2.5 μg/mL insulin was used. After 4 days, cell aggregates were grown in neuronal differentiation media, composed as aforementioned except by replacing with 1X B27 containing vitamin A (Gibco). The medium was changed once per week. Cerebral organoids were grown for 45 days (30 days in neuronal differentiation media).

RNA isolation and PCR analysis. Total RNA was isolated using the GeneJET RNA Purification Kit (Thermo Scientific) and digested with DNase using DNase I (Invitrogen), following the manufacturer's instructions. Complementary DNA was generated from 1 μg total RNA using M-MLV Reverse Transcriptase (Invitrogen), according to the manufacturer's recommendations. PCR was performed using the following primer sequences: GFAP-For: 5′-TTC GAC AGT CAG CCG CAT C-3′ GFAP-Rev: 5′-GAC TCC ACG ACG TAC TCA GC-3′, Sigma receptor 1-For: 5′-AGT AGG ACC ATG CAC TCA CAC C-3′, Sigma receptor 1-Rev: 5′-CCC CAT CCT TAA CTC TAG AAC C-3′, 5-HT_{2A}-For: 5′-TTG GGC TAC AGG ACG ATT-3′, 5-HT_{2A}-Rev: 5′-GAA GAA AGG GCA CCA CAT C-3′, 5-HT_{2C}-For: 5′-TGT CCC TAG CCA TTG CTG ATA TGC-3′, 5-HT_{2C}-Rev: 5′-GCA ATC TTC ATG ATG GCC TTA GTC-3′. Each PCR reaction was carried out for 40 cycles in a reaction mixture containing 0.25 U Taq DNA Polymerase (Invitrogen), 1x Taq DNA Polymerase Buffer containing 1.5 mM $MgCl_2$ (Invitrogen), 200 nM of each primer (forward and reverse), 200 μM dNTP mixture containing the four deoxyribonucleotides (dATP, dCTP, dTTP, dGTP), and 15 ng of cDNA.

Immunohistochemistry. On the 45th day of differentiation, cerebral organoids were fixed in 4% paraformaldehyde, incubated with sucrose solutions (10, 20, and 30%) in phosphate buffered saline (PBS), embedded in optimal cutting temperature compound (OCT), and frozen in liquid nitrogen. The organoids were sectioned with a cryostat into 20 μm thick sections. Immunofluorescence was performed using the primary antibodies: anti-MAP2 (M1406, Sigma-Aldrich), anti-AMPAR1 (Abcam, ab86141), anti-NMDAR1 (Abcam, ab28669), anti-sigma receptor 1 (sc-137075, Santa Cruz), and anti-5-HT_{2A} receptor (RA24288, Neuromics). Secondary antibodies used were as follows: Alexa Fluor 488 goat anti-mouse (A11001, Invitrogen) and Alexa Fluor 594 goat anti-mouse (A-11008, Invitrogen). DAPI was used for nucleus staining. Images were acquired using an Operetta Imaging System (Perkin Elmer) and a Leica TCS SP8 confocal microscope, when specified.

Treatment of cerebral organoids with 5-MeO-DMT. On day 45 of differentiation, four to five organoids per group were transferred from the spinner flask to a non-adherent dish and treated with either 13 μM 5-MeO-DMT (Sigma-Aldrich), 0.3% ethanol (vehicle) or only medium (control), for 24 hours. After treatment, cerebral organoids were pelleted and homogenized in buffer containing 7 M Urea, 2 M thiourea, 4% CHAPS, 70 mM DTT, and Complete Protease Inhibitor Cocktail (Roche)[80]. The homogenates were kept on ice for about 20 min and frozen at −80 °C until sample processing for mass spectrometry-based label-free shotgun proteomics. The experiment was repeated three times with the three different derivations of cerebral organoids.

Sample preparation. Sample lysates were thawed and centrifuged at 10,000 × g for 10 min at 4 °C. The supernatant was collected and total protein was quantified by Qubit® 3.0 Fluorometer (Thermo Fisher Scientific). Each sample (50 μg) was subjected to a SDS-PAGE gel electrophoresis. Gel lanes were sliced and digested *in gel* overnight as previously described[80]. Generated peptides were dried in a SpeedVac concentrator and stored at −80 °C prior to shotgun mass spectrometry analyses.

Liquid chromatography-mass spectrometry. Qualitative and quantitative proteomic analyses were performed on a 2D-LC-MS/MS system with ion-mobility-enhanced, data-independent acquisitions[81]. Peptides were injected for two-dimensional, reverse-phase liquid chromatography using an Acquity UPLC M-Class System (Waters Corporation, Milford, MA) coupled to a Synapt G2-Si mass spectrometer (Waters Corporation, Milford, MA).

In first-dimension chromatography, peptides (5 μg) were loaded into a M-Class BEH C18 Column (130 Å, 5 μm, 300 μm × 50 mm, Waters Corporation, Milford, MA). Fractionation was performed using discontinuous steps of acetonitrile (11%, 14%, 17%, 20%, and 50%). After each step, peptide loads continued to second-dimension separation, in a nanoACQUITY UPLC HSS T3 Column (100 Å, 1.8 μm, 75 μm × 150 mm, Waters Corporation, Milford, MA). Peptide elution was achieved using an acetonitrile gradient from 7% to 40% (v/v) for 54 min at a flow rate of 0.4 μL/min directly into a Synapt G2-Si. The mass spectrometer acquired in data-independent acquisition mode (DIA) with ion-mobility separation. This approach, called high-definition data-independent mass spectrometry ($HDMS^E$), significantly enhances the proteome coverage[82]. MS/MS analyses were performed by nano-electrospray ionization in positive ion mode, nanoESI (+), and used a NanoLock Spray (Waters, Manchester, UK) ionization source. The lock mass channel was sampled every 30 s. The mass spectrometer was calibrated with an MS/MS spectrum of a [Glu1]-Fibrinopeptide B human (Glu-Fib) solution that was delivered through the reference sprayer of the NanoLock Spray source. Samples were all run in technical and biological triplicates, for a total of 9 replicates per sample.

Database search and quantification. Raw data was processed with Progenesis® QI version 2.1 (Waters) and proteins were identified. Quantitative data was processed using dedicated algorithms and searched against

the Uniprot human proteomics database (version 2015/09), with the default parameters for ion accounting and quantitation[83]. The databases used were reversed "on the fly" during the database queries and appended to the original database to assess the false-positive identification rate. The following parameters were considered in identifying peptides: 1) Digestion by trypsin with at most one missed cleavage; 2) variable modifications by oxidation (M) and fixed modification by carbamidomethyl (C); and 3) false discovery rate (FDR) less than 1%. Identifications that did not satisfy these criteria were not considered.

***In silico* analysis.** Protein networks and canonical pathways associated with differentially expressed proteins were identified using Ingenuity Pathway Analysis software (IPA, Ingenuity Systems, Qiagen, Redwood, CA, USA; www.ingenuity.com). This software uses curated connectivity information from literature to determine interaction networks among the differentially expressed proteins and canonical pathways in which they are involved. Here, we have considered information from nervous system tissues and cells, immune cells, and stem cells. The significant biological functions were based on Fisher's exact test. Multiple correlation hypotheses were based on Benjamini-Hochberg (B-H) approach using a 1% FDR threshold; the significance of the IPA test was expressed as p-values.

References

1. Barker, S. A., McIlhenny, E. H. & Strassman, R. A critical review of reports of endogenous psychedelic N, N-dimethyltryptamines in humans: 1955–2010. *Drug Test Anal* **4**, 617–635 (2012).
2. Strassman, R. DMT: The spirit molecule (2001).
3. McKenna, D. J. Clinical investigations of the therapeutic potential of ayahuasca: rationale and regulatory challenges. *Pharmacol. Ther.* **102**, 111–129 (2004).
4. Ott, J. Pharmañopo-psychonautics: human intranasal, sublingual, intrarectal, pulmonary and oral pharmacology of bufotenine. *J Psychoactive Drugs* **33**, 273–281 (2001).
5. Holmstedt, B. & Lindgren, J. Chemical constituents and pharmacology of South American snuffs. *Psychopharmacol Bull* **4**, 16 (1967).
6. Labate, B. C. & Feeney, K. Ayahuasca and the process of regulation in Brazil and internationally: implications and challenges. *Int. J. Drug Policy* **23**, 154–161 (2012).
7. Osório, F. de, L. *et al*. Antidepressant effects of a single dose of ayahuasca in patients with recurrent depression: a preliminary report. *Rev. Bras. Psiquiatr.* **37**, 13–20 (2015).
8. Sanches, R. F. *et al*. Antidepressant Effects of a Single Dose of Ayahuasca in Patients With Recurrent Depression. *Journal of Clinical Psychopharmacology* **36**, 77–81 (2016).
9. Bouso, J. C. *et al*. Personality, Psychopathology, Life Attitudes and Neuropsychological Performance among Ritual Users of Ayahuasca: A Longitudinal Study. *PLoS ONE* **7**, e42421 EP (2012).
10. Bouso, J. C. *et al*. Long-term use of psychedelic drugs is associated with differences in brain structure and personality in humans. *Eur Neuropsychopharmacol* **25**, 483–492 (2015).
11. Shen, H. W., Jiang, X. L. & Winter, J. C. Psychedelic 5-methoxy-N, N-dimethyltryptamine: metabolism, pharmacokinetics, drug interactions, and pharmacological actions. *Current Drug Metabolism* **11**, 659–666 (2010).
12. Weil, A. T. & Davis, W. Bufo alvarius: a potent hallucinogen of animal origin. *J Ethnopharmacol* **41**, 1–8 (1994).
13. Fontanilla, D. *et al*. The hallucinogen N,N-dimethyltryptamine (DMT) is an endogenous sigma-1 receptor regulator. *Science* **323**, 934–937 (2009).
14. Szabo, A., Kovacs, A., Frecska, E. & Rajnavolgyi, E. Psychedelic N,N-Dimethyltryptamine and 5-Methoxy-N,N-Dimethyltryptamine Modulate Innate and Adaptive Inflammatory Responses through the Sigma-1 Receptor of Human Monocyte-Derived Dendritic Cells. *PLoS ONE* **9**, e106533 EP – (2014).
15. Szabo, A. *et al*. The Endogenous Hallucinogen and Trace Amine N,N-Dimethyltryptamine (DMT) Displays Potent Protective Effects against Hypoxia via Sigma-1 Receptor Activation in Human Primary iPSC-Derived Cortical Neurons and Microglia-Like Immune Cells. *Front Neurosci* **10**, 423 (2016).
16. Oliveira-Lima, A. J. *et al*. Effects of ayahuasca on the development of ethanol-induced behavioral sensitization and on a post-sensitization treatment in mice. *Physiol. Behav.* **142**, 28–36 (2015).
17. Nutt, D. J., King, L. A. & Nichols, D. E. Effects of Schedule I drug laws on neuroscience research and treatment innovation. *Nat Rev Neurosci* **14**, 577–585 (2013).
18. Hanks, J. B. & González-Maeso, J. Animal models of serotonergic psychedelics. *ACS Chem Neurosci* **4**, 33–42 (2013).
19. la Torre, deR. & Farré, M. Neurotoxicity of MDMA (ecstasy): the limitations of scaling from animals to humans. *Trends in Pharmacological Sciences* **25**, 505–508 (2004).
20. Vollenweider, F. X. & Kometer, M. The neurobiology of psychedelic drugs: implications for the treatment of mood disorders. *Nat Rev Neurosci* **11**, 642–651 (2010).
21. Kelava, I. & Lancaster, M. A. Stem Cell Models of Human Brain Development. *Cell Stem Cell* **18**, 736–748 (2016).
22. Lancaster, M. A. & Knoblich, J. A. Generation of cerebral organoids from human pluripotent stem cells. *Nat Protoc* **9**, 2329–2340 (2014).
23. Qian, X. *et al*. Brain-Region-Specific Organoids Using Mini- bioreactors for Modeling ZIKV Exposure. *Cell* **0**, 1–18 (2016).
24. Camp, J. G. *et al*. Human cerebral organoids recapitulate gene expression programs of fetal neocortex development. *Proc Natl Acad Sci USA* **112**, 15672–15677 (2015).
25. Garcez, P. P. *et al*. Zika virus impairs growth in human neurospheres and brain organoids. *Science* **352**, 816–818 (2016).
26. Lancaster, M. A. *et al*. Cerebral organoids model human brain development and microcephaly. *Nature* **501**, 373–379 (2013).
27. Martins-de-Souza, D. Proteomics Tackling Schizophrenia as a Pathway Disorder. *Schizophrenia Bulletin* **38**, 1107–1108 (2012).
28. Dakic, V. *et al*. Harmine stimulates proliferation of human neural progenitors. *PeerJ* **4**, e2727 (2016).
29. Sartore, R. C. *et al*. Trace elements during primordial plexiform network formation in human cerebral organoids. *PeerJ* **5**, e2927 (2016).
30. Malenka, R. C. & Bear, M. F. LTP and LTD: an embarrassment of riches. *Neuron* **44**, 5–21 (2004).
31. Alberini, C. M. Transcription factors in long-term memory and synaptic plasticity. *Physiol. Rev.* **89**, 121–145 (2009).
32. Boyd, A. W., Bartlett, P. F. & Lackmann, M. Therapeutic targeting of EPH receptors and their ligands. *Nat Rev Drug Discov* **13**, 39–62 (2014).
33. House, R. V., Thomas, P. T. & Bhargava, H. N. Immunological consequences of *in vitro* exposure to lysergic acid diethylamide (LSD). *Immunopharmacol Immunotoxicol* **16**, 23–40 (1994).
34. Voss, E. W. & Winkelhake, J. L. Mechanism of lysergic acid diethylamide interference with rabbit antibody biosynthesis. *Proc. Natl. Acad. Sci. USA* **71**, 1061–1064 (1974).
35. Boyle, N. T. & Connor, T. J. Methylenedioxymethamphetamine ('Ecstasy')-induced immunosuppression: a cause for concern? *Br J Pharmacol* **161**, 17–32 (2010).

36. Connor, T. J., Kelly, J. P., McGee, M. & Leonard, B. E. Methylenedioxymethamphetamine (MDMA; Ecstasy) suppresses IL-1beta and TNF-alpha secretion following an *in vivo* lipopolysaccharide challenge. *Life Sciences* **67**, 1601–1612 (2000).
37. Nau, F., Yu, B., Martin, D. & Nichols, C. D. Serotonin 5-HT2A receptor activation blocks TNF-α mediated inflammation *in vivo*. *PLoS ONE* **8**, e75426 (2013).
38. Yu, B. *et al*. Serotonin 5-hydroxytryptamine(2A) receptor activation suppresses tumor necrosis factor-alpha-induced inflammation with extraordinary potency. *Journal of Pharmacology and Experimental Therapeutics* **327**, 316–323 (2008).
39. Szabo, A. Psychedelics and Immunomodulation: Novel Approaches and Therapeutic Opportunities. *Front Immunol* **6**, 358 (2015).
40. Chiamulera, C. *et al*. Reinforcing and locomotor stimulant effects of cocaine are absent in mGluR5 null mutant mice. *Nat Neurosci* **4**, 873–874 (2001).
41. Stoker, A. K., Olivier, B. & Markou, A. Involvement of metabotropic glutamate receptor 5 in brain reward deficits associated with cocaine and nicotine withdrawal and somatic signs of nicotine withdrawal. *Psychopharmacology (Berl.)* **221**, 317–327 (2012).
42. Bird, M. K., Kirchhoff, J., Djouma, E. & Lawrence, A. J. Metabotropic glutamate 5 receptors regulate sensitivity to ethanol in mice. *Int. J. Neuropsychopharmacol.* **11**, 765–774 (2008).
43. Barbosa, P. C. R., Mizumoto, S., Bogenschutz, M. P. & Strassman, R. J. Health status of ayahuasca users. *Drug Test Anal* **4**, 601–609 (2012).
44. Crews, F. T., Zou, J. & Qin, L. Induction of innate immune genes in brain create the neurobiology of addiction. *Brain, Behavior, and Immunity* **25**(Suppl 1), S4–S12 (2011).
45. Doering-Silveira, E. *et al*. Report on psychoactive drug use among adolescents using ayahuasca within a religious context. *J Psychoactive Drugs* **37**, 141–144 (2005).
46. Fábregas, J. M. *et al*. Assessment of addiction severity among ritual users of ayahuasca. *Drug Alcohol Depend* **111**, 257–261 (2010).
47. Thomas, G., Lucas, P., Capler, N. R., Tupper, K. W. & Martin, G. Ayahuasca-assisted therapy for addiction: results from a preliminary observational study in Canada. *Curr Drug Abuse Rev* **6**, 30–42 (2013).
48. Barbanoj, M. J. *et al*. Daytime Ayahuasca administration modulates REM and slow-wave sleep in healthy volunteers. *Psychopharmacology (Berl.)* **196**, 315–326 (2008).
49. Blanco, W. *et al*. Synaptic Homeostasis and Restructuring across the Sleep-Wake Cycle. *PLoS Computational Biology* **11**, e1004241 (2015).
50. Dumoulin Bridi, M. C. *et al*. Rapid eye movement sleep promotes cortical plasticity in the developing brain. *Sci Adv* **1**, e1500105 (2015).
51. Tononi, G. & Cirelli, C. Sleep and the Price of Plasticity: From Synaptic and Cellular Homeostasis to Memory Consolidation and Integration. *Neuron* **81**, 12–34 (2014).
52. Ribeiro, S. Sleep and plasticity. *Pflugers Arch - Eur J Physiol* **463**, 111–120 (2012).
53. Bourne, J. N. & Harris, K. M. Balancing structure and function at hippocampal dendritic spines. *Annu Rev Neurosci* (2008).
54. Jones, K. A. *et al*. Rapid modulation of spine morphology by the 5-HT2A serotonin receptor through kalirin-7 signaling. *Proc Natl Acad Sci USA* **106**, 19575–19580 (2009).
55. Klein, R. Bidirectional modulation of synaptic functions by Eph/ephrin signaling. *Nat Neurosci* **12**, 15–20 (2009).
56. Irie, F. & Yamaguchi, Y. EphB receptors regulate dendritic spine development via intersectin, Cdc42 and N-WASP. *Nat Neurosci* **5**, 1117–1118 (2002).
57. Takenawa, T. & Miki, H. WASP and WAVE family proteins: key molecules for rapid rearrangement of cortical actin filaments and cell movement. *J Cell Sci* **114**, 1801–1809 (2001).
58. Henkemeyer, M., Itkis, O. S., Ngo, M., Hickmott, P. W. & Ethell, I. M. Multiple EphB receptor tyrosine kinases shape dendritic spines in the hippocampus. *J Cell Biol* **163**, 1313–1326 (2003).
59. Kayser, M. S., McClelland, A. C., Hughes, E. G. & Dalva, M. B. Intracellular and trans-synaptic regulation of glutamatergic synaptogenesis by EphB receptors. *Journal of Neuroscience* **26**, 12152–12164 (2006).
60. Takasu, M. A., Dalva, M. B., Zigmond, R. E. & Greenberg, M. E. Modulation of NMDA receptor-dependent calcium influx and gene expression through EphB receptors. *Science* **295**, 491–495 (2002).
61. Ruscher, K. *et al*. The sigma-1 receptor enhances brain plasticity and functional recovery after experimental stroke. *Brain* **134**, 732–746 (2011).
62. Tsai, S.-Y. *et al*. Sigma-1 receptors regulate hippocampal dendritic spine formation via a free radical-sensitive mechanism involving Rac1xGTP pathway. *Proc Natl Acad Sci USA* **106**, 22468–22473 (2009).
63. Griffiths, R. R., Richards, W. A., McCann, U. & Jesse, R. Psilocybin can occasion mystical-type experiences having substantial and sustained personal meaning and spiritual significance. *Psychopharmacology (Berl.)* **187**, 268–83 discussion 284–92 (2006).
64. Quadrato, G. *et al*. Cell diversity and network dynamics in photosensitive human brain organoids. *Nature* **545**, 48–53 (2017).
65. Laht, P., Otsus, M., Remm, J. & Veske, A. B-plexins control microtubule dynamics and dendrite morphology of hippocampal neurons. *Exp Cell Res* **326**, 174–184 (2014).
66. Horn, K. E. *et al*. DCC expression by neurons regulates synaptic plasticity in the adult brain. *Cell Reports* **3**, 173–185 (2013).
67. Bozdagi, O., Nagy, V., Kwei, K. T. & Huntley, G. W. *In vivo* roles for matrix metalloproteinase-9 in mature hippocampal synaptic physiology and plasticity. *J. Neurophysiol.* **98**, 334–344 (2007).
68. Dityatev, A. & Schachner, M. The extracellular matrix and synapses. *Cell Tissue Res* **326**, 647–654 (2006).
69. Shi, Y. & Ethell, I. M. Integrins Control Dendritic Spine Plasticity in Hippocampal Neurons through NMDA Receptor and Ca2+/Calmodulin-Dependent Protein Kinase II-Mediated Actin Reorganization. *J. Neurosci.* **26**, 1813–1822 (2006).
70. Martins-de-Souza, D. *et al*. Blood Mononuclear Cell Proteome Suggests Integrin and Ras Signaling as Critical Pathways for Antidepressant Treatment Response. *Biol. Psychiatry*, https://doi.org/10.1016/j.biopsych.2014.01.022 (2014).
71. Endris, V. *et al*. The novel Rho-GTPase activating gene MEGAP/ srGAP3 has a putative role in severe mental retardation. *Proc. Natl. Acad. Sci. USA* **99**, 11754–11759 (2002).
72. Frecska, E., Szabo, A., Winkelman, M. J., Luna, L. E. & McKenna, D. J. A possibly sigma-1 receptor mediated role of dimethyltryptamine in tissue protection, regeneration, and immunity. *J Neural Transm* **120**, 1295–1303 (2013).
73. Mueller, B. H. *et al*. Sigma-1 receptor stimulation attenuates calcium influx through activated L-type Voltage Gated Calcium Channels in purified retinal ganglion cells. *Exp. Eye Res.* **107**, 21–31 (2013).
74. Tchedre, K. T. & Yorio, T. sigma-1 receptors protect RGC-5 cells from apoptosis by regulating intracellular calcium, Bax levels, and caspase-3 activation. *Invest Ophthalmol Vis Sci* **49**, 2577–2588 (2008).
75. Duman, R. S., Aghajanian, G. K., Sanacora, G. & Krystal, J. H. Synaptic plasticity and depression: new insights from stress and rapid-acting antidepressants. *Nat Med* **22**, 238–249 (2016).
76. Duman, R. S. & Aghajanian, G. K. Synaptic Dysfunction in Depression: Potential Therapeutic Targets. *Science* **338**, 68 (2012).
77. Gerhard, D. M., Wohleb, E. S. & Duman, R. S. Emerging treatment mechanisms for depression: focus on glutamate and synaptic plasticity. *Drug Discov. Today* **21**, 454–464 (2016).
78. Fraga, A. M. *et al*. Establishment of a Brazilian Line of Human Embryonic Stem Cells in Defined Medium: Implications for Cell Therapy in an Ethnically Diverse Population. *Cell Transplant* **20**, 431–440 (2011).
79. Baharvand, H. *et al*. Neural differentiation from human embryonic stem cells in a defined adherent culture condition. *Int. J. Dev. Biol.* **51**, 371–378 (2007).
80. Maccarrone, G., Lebar, M. & Martins-de-Souza, D. Brain quantitative proteomics combining GeLC-MS and isotope-coded protein labeling (ICPL). *Methods Mol. Biol.* **1156**, 175–185 (2014).

81. Souza, G. H. M. F., Guest, P. C. & Martins-de-Souza, D. LC-MS(E), Multiplex MS/MS, Ion Mobility, and Label-Free Quantitation in Clinical Proteomics. *Methods Mol. Biol.* **1546**, 57–73 (2017).
82. Distler, U. *et al*. Drift time-specific collision energies enable deep-coverage data-independent acquisition proteomics. *Nat Meth* **11**, 167–170 (2013).
83. Li, C. *et al*. SubpathwayMiner: a software package for flexible identification of pathways. *Nucleic Acids Res* **37**, e131–e131 (2009).

Acknowledgements

This work is part of the PhD thesis of VD. We thank Yury M. Lages, Dr. Sylvie Devalle, Ismael Gomes, Marcelo Costa and Gabriela Vitoria for technical assistance, and Bradley Joseph Smith for English editing. We also would like to thank Dr. Richardson Leão, Dr. Marília Zaluar Passos Guimarães and Dr. Eduardo Schenberg for their support during this project. This study was funded by the following Brazilian funding agencies: National Council for Scientific and Technological Development (CNPq), Foundation for Research Support in the State of Rio de Janeiro (FAPERJ), Coordenação de Aperfeiçoamento de Pessoal de Nível Superior (CAPES), Funding Authority for Studies and Projects (FINEP), Brazilian Development Bank (BNDES) and São Paulo Research Foundation (grants 2013/08711-3, 2014/10068-4 and 2014/21035-0). The funders had no role in study design, data collection, or analysis, nor had they influence on the preparation of the manuscript or the decision to publish it.

Author Contributions

V.D., J.M.N., S.K.R. designed the experiments; V.D., J.M.N., R.M.M., R.S. performed the experiments; D.M.S. supervised analysis and interpretation of the proteomics data; V.D., J.M.N., and R.M.M. analyzed the data; V.D., J.M.N., S.K.R. wrote the paper; V.D., J.M.N., R.M.M., R.S. prepared figures; V.D., J.M.N., R.M.M., R.S., D.A., S.R., D.M.S., S.K.R. reviewed drafts of the paper.

Additional Information

Supplementary information accompanies this paper at https://doi.org/10.1038/s41598-017-12779-5.

Competing Interests: The authors declare that they have no competing interests.

Publisher's note: Springer Nature remains neutral with regard to jurisdictional claims in published maps and institutional affiliations.